Ambiente & Água - An Interdisciplinary Journal of Applied Science
ISSN 1980-993X – doi:10.4136/1980-993X
www.ambi-agua.net
E-mail: ambi.agua@gmail.com

CWSI and soil matric potential as indicators to optimize irrigation in common bean production in different soil types

ARTICLES doi:10.4136/ambi-agua.3114

Received: 01 Sep. 2025; Accepted: 22 Apr. 2026

Thatyane Kary Grigório de Souza; João José da Silva Junior*; Filipe Bittencourt Machado de Souza

Faculdade de Agronomia e Medicina Veterinária. Universidade de Brasília (UnB), Campus Darcy Ribeiro, Asa Norte, CEP: 70910-900, Brasília, DF, Brazil. E-mail: thatyanekary@usp.br, fbmsouza@yahoo.com.br
*Corresponding author. E-mail: jjsjunior@unb.br
Editor-in-Chief: Nelson Wellausen Dias

ABSTRACT
To optimize water usage and increase production, it is important to use efficient irrigation control and management systems. The crop water stress index (CWSI) and soil matric potential have emerged as promising alternatives for irrigation management. In a greenhouse experiment, different irrigation rates were applied to two types of soil (Red Latosol and Red-Yellow Latosol) based on various water tensions (-10, -20, -25, -30, and -40 kPa). The experiment was conducted in a completely randomized design (CRD), in a 5x2 factorial arrangement (five soil water tension levels and two soil types), with four replications. Soil matric potential (SMP) and crop water stress index (CWSI) were evaluated, calculated from thermal images of common bean plants and meteorological data. Linear and non-linear relationships between these stress indicators were analyzed at different crop growth stages. The CWSI based on canopy temperature is an effective tool for determining irrigation requirements for beans at different growth stages. Linear and quadratic regressions were obtained between soil matric potential and CWSI for Red Latosol at growth stage R7 and for Red-Yellow Latosol at stages R5 to R8.

Keywords: canopy temperature, thermal imaging, water deficit.

CWSI e potencial mátrico do solo como indicadores para otimizar a irrigação na produção de feijão comum em diferentes tipos de solo

RESUMO
Para otimizar o uso da água e aumentar a produção, é importante utilizar sistemas eficientes de controle e manejo da irrigação. O índice de estresse hídrico da cultura (CWSI) e o potencial matricial do solo têm se destacado como alternativas promissoras para o manejo da irrigação. Em um experimento conduzido em casa de vegetação, diferentes lâminas de irrigação foram aplicadas a dois tipos de solo (Latossolo Vermelho e Latossolo Vermelho-Amarelo), com base em diferentes tensões hídricas (-10, -20, -25, -30 e -40 kPa). O experimento foi conduzido em delineamento inteiramente casualizado (DIC), em arranjo fatorial 5×2 (cinco níveis de tensão hídrica do solo e dois tipos de solo), com quatro repetições. Foram avaliados o potencial matricial do solo (PMS) e o índice de estresse hídrico da cultura (CWSI), calculados a partir de imagens térmicas de plantas de feijão comum e dados meteorológicos. As relações lineares e

não lineares entre esses indicadores de estresse foram analisadas em diferentes estádios de desenvolvimento da cultura. O CWSI baseado na temperatura do dossel mostrou-se uma ferramenta eficaz para determinar as necessidades de irrigação do feijoeiro em diferentes estádios de crescimento. Regressões lineares e quadráticas foram obtidas entre o potencial matricial do solo e o CWSI para o Latossolo Vermelho no estádio de crescimento R7 e para o Latossolo Vermelho-Amarelo nos estádios R5 a R8.

Palavras-chave: déficit hídrico, imageamento térmico, temperatura do dossel.

1. INTRODUCTION

Common beans (*Phaseolus vulgaris* L.) are highly important in Brazil due to their popularity as a staple food and main source of protein in the population's diet. Conab reports that in the 2023/2024 harvest, bean production was 3.1 million tons and the total planted area was 2.8 million hectares. The crop has a short cycle, low sensitivity to photoperiod variations, and can be produced throughout the year, even in the driest period, between July and October, where around 694.9 thousand tons were produced using center pivot irrigation in 2023 (CONAB, 2023). Therefore, evaluating cultivation systems and management techniques that can boost crop production, such as irrigation, is crucial, particularly due to the scarcity of water resources.

In this context, reliable indicators of plant water status are necessary to support irrigation management and optimize water use in agricultural systems. One of the most widely used indicators for assessing plant water stress is the crop water stress index (CWSI), originally proposed by Idso *et al.* (1981) and later modified by Jackson *et al.* (1981). This index is based on the difference between leaf temperature and air temperature, derived from the Penman Monteith equation and the energy balance equation. The minimum and maximum limits of this difference are called the lower baseline (LBI) and upper baseline (LBS), respectively.

In an experiment with cotton, Padhi *et al.* (2012) tested whether infrared thermography could distinguish systematic variation in irrigation. They found that canopy temperature measured using thermal images can be reliably associated with environmental parameters and the stomatal conductance index related to plant water tension. The authors suggest that the use of the water stress index obtained by thermography is an efficient tool for managing cotton irrigation.

Bellvert *et al.* (2014) used an unmanned aerial vehicle to obtain thermal images of vines and compared them with temperatures obtained from an infrared thermometer to determine the CWSI in vines with and without water restrictions for two consecutive years: 2009 and 2010. They found good correlations between leaf water potential and the water stress index of the vines in both situations. The authors concluded that the two methods are efficient in determining the variability of water stress in these plants.

Lobo *et al.* (2004) concluded that the bean crop should receive water whenever the leaf temperature of a plant without water restriction is 3 to 4ºC warmer than the plant under study. Gonzalez-Dugo *et al.* (2013) state that temperature-based indicators of crop water stress are inversely related to transpiration rate and stomatal conductance and have been successfully related to indicators of crop water status, such as leaf water potential.

Oliveira *et al.* (2009) suggest that it is possible to define when to proceed with irrigation by associating the water potential of the leaves with the matric potential of the soil by adjusting models. This can be done by using the water retention curve in the soil to determine the level to be applied. Optimization of water use and irrigation management in bean crops in Brazil is important for both environmental and economic goals. Thus, this study aims to obtain equations that correlate the soil matric potential with the CWSI for each phenological stage of the common bean in Red Latosol and Yellow Red Latosol, which can help with irrigation management in the bean crop using thermometry and the soil water retention curve.

2.MATERIAL AND METHODS

The experiment was conducted in a greenhouse located at the Experimental Biological Station, on the Darcy Ribeiro Campus (DF) of the University of Brasília (15°44'S; 47°52'W). According to the Köppen-Geiger classification, the climate of the region is tropical (Aw), with a dry season in winter. Average annual precipitation is 1360 mm, and average annual maximum and minimum temperatures are 26.7°C and 16.1°C.

The greenhouse (30 m × 13 m) is equipped with an evaporative air-cooling system composed of an expanded clay panel with a motor pump used to hold water to the upper part of the panel. In addition, eight exhaust fans with an individual removal capacity of 450 m³ air min^{-1} were installed on the opposite side of the expanded clay panel for optimal removal of moisture in the interior air. The activation control of the cooling system was based on the interior air temperature, adjusted by a thermostat at 27°C installed in the central part of the greenhouse at 2 m from the ground (Pereira, 2021). The greenhouse rooftop is made of a transparent plastic cover (diffuser film) and black screen cover, whereas the sides are made of asbestos tiles. For the specific experiment, the black screen was removed to reduce shading on the plants because the bean crop is not very sensitive to solar radiation.

In a greenhouse experiment, different irrigation rates were applied to two types of soil (Red Latosol and Red-Yellow Latosol) based on various water tensions (-10, -20, -25, -30, and -40 kPa). The experiment was conducted in a completely randomized design (CRD), in a 5x2 factorial arrangement (five soil water tension levels and two soil types), with four replications. Soil matric potential (SMP) and crop water stress index (CWSI) were evaluated, calculated from thermal images of common bean plants and meteorological data. The pots were placed in the greenhouse along ten rows. Rows were 1.0 m apart, whereas pots were 0.4 m apart along the rows, for a total of 80 pots. Half of the pots were used as a buffer zone. Pots were placed on 9-hole bricks to avoid direct contact with the floor, thus minimizing disease transmission.

Climatological data during the crop cycle were obtained using a 900 ET WatchDog weather station (*Spectrum Technologies*) installed inside the greenhouse. The station records air relative humidity (%), air temperature (°C), solar radiation ($W\ m^{-2}$), wind speed ($m\ s^{-1}$) and direction (°), wind chill (°C) and dew point (°C).

The common bean (*Phaseolus vulgaris* L.), cultivar BRSFC 104, was seeded on May 25th, 2021, at a depth of 3 cm. The experiment was conducted in 11 L plastic pots filled with a Red Latosol (Oxisol) and Red-Yellow collected from an experimental field (see below for details). In the inner base of each pot, we placed a synthetic non-woven mat, and 2 cm of gravel was added over the mat for drainage. Four seeds were sown per pot, but only two plants were kept after emergence, for a total of 40 plants.

Control of weeds, pests and diseases was carried out when necessary. The seeds were treated with the Maxim X fungicide, which contains active ingredients such as mefenoxam and fludioxonil. Two applications of a fungicide that contains the active ingredient mancozeb (750 $g\ kg^{-1}$) at a concentration of 0.4 $g\ L^{-1}$ were applied at 24 and 45 days after emergence (DAE). Deltamethrin (25 $g\ L^{-1}$) at a concentration of 0.08 $mL\ L^{-1}$ and neem oil at 4 $mL\ L^{-1}$were also applied to control insects on 39 and 34 DAE, respectively.

The Red Latosol (Oxisol) and Red-Yellow Latosol were first collected at the Água Limpa Farm, FAV/UnB experimental field. Following physical and chemical characterization of the soils (Table 1), they were fertilized to correct pH and any nutrient imbalances according to Embrapa recommendations for Cerrado soils. Fertilization was carried out manually in each pot, converting the amounts recommended for a broadcast (field) application ($kg\ ha^{-1}$) to a pot application representing a surface area of 530 cm^{-2} ($g\ pot^{-1}$). For soil pH correction, magnesian limestone was used, whereas potassium and phosphorus were added using potassium chloride (KCl) and Yoorin Master (P_2O_5) fertilizers. Nitrogen was added in three applications, one during seeding and two at top-dressing using urea ($CO(NH_2)_2$) (Table 2).

Table 1. Chemical and physical characteristics of the first twenty centimeters of Red Latosol (Oxisol) and Red-Yellow Latosol.

	pH	P	K	Ca	Mg	Na	Al	(H + Al)	BS	CEC
Red Latosol	15.2	0.09	2.40	0.40	0.11	0.30	3.40	3.00	6.40	15.2
Red-Yellow Latosol	1.10	0.14	2.10	0.50	0.15	0.10	3.20	2.90	6.10	1.10
	V	M	ISNa	C	MO	Clay	Silt	Sand	Ds	Pt
Red Latosol	47.0	9.00	4.00	20.0	34.4	72.7	25.1	2.20	0.94	0.64
Red-Yellow Latosol	47.0	3.00	5.00	11.0	18.9	59.2	36.7	4.10	1.00	0.62

pH is in H_2O; P (Mehlich), Ca, Mg, K, Na, Al are exchangeable phosphorus, calcium, magnesium, potassium, sodium and aluminum, respectively ($cmol_+ \ dm^{-3}$); (H+Al) is exchangeable acidity ($cmol_+ \ dm^{-3}$); BS is the sum of exchangeable base cations ($cmol_+ \ dm^{-3}$); CEC is cation exchange capacity ($cmol_c \ dm^{-3}$); V is base saturation (%) calculated as BS on CEC; M is aluminum saturation (%) calculated as exchangeable Al on CEC; ISNa is sodium saturation (%) calculated as exchangeable Na on CEC; C is organic carbon ($g \ kg^{-1}$); MO is organic matter ($g \ kg^{-1}$); Ds is density; and Pt is porosity.

Table 2. Liming and fertilizer application rates by broadcast (field) per pot for the Red Latosol (LR) and Red-Yellow Latosol (LRY).

nutrients	Recommendation (broadcast application, kg ha^{-1})		Application per pot (g)		Sowing	top-dressing	
						1st application	2nd application
	LR	LRY	LR	LRY			
Magnesian limestone	4.58	4.37	-	-			
No	100	100	1.16	1.16	20%	40%	40%
P_2O_5	150	420	1.88	13.2	100%	-	-
K_2O	60	100	1.18	0.72	60%	40%	-

The automated irrigation system consisted of a water pump coupled with two 500 L water tanks. Irrigation was carried out using a drip system (i.e., dripper per button type in each pot), composed of one regulator valve system. The irrigation system was composed of five regulator valve systems, one per water tension. Flow rates were adjusted to create five soil water tension treatments at -10, -20, -25, -30, and -40 kPa. In the first 22 days following seeding, all pots received 3 minutes of irrigation at a nominal rate of 1 L h^{-1}. This procedure warranted seed germination and uniform seedlings before the onset of the water deficit treatments. The measurement of soil water tension started 18 days after seedling emergence. Soil water tension was monitored using puncture tensiometers with a digital pressure gauge. Soil water tension was measured in all 40 pots at a 10 cm depth. Measurements were carried out on alternate days between 11:30 am and 1:30 pm. We used the soil water retention curves (Figure 1) of Pereira (2021) who used the Van Genuchten (1980) model. The SMP and water retention curves were then used to determine the water depths to be applied for each soil type (Equation 1) and the time required to complete water application to these depths (Equation 2).

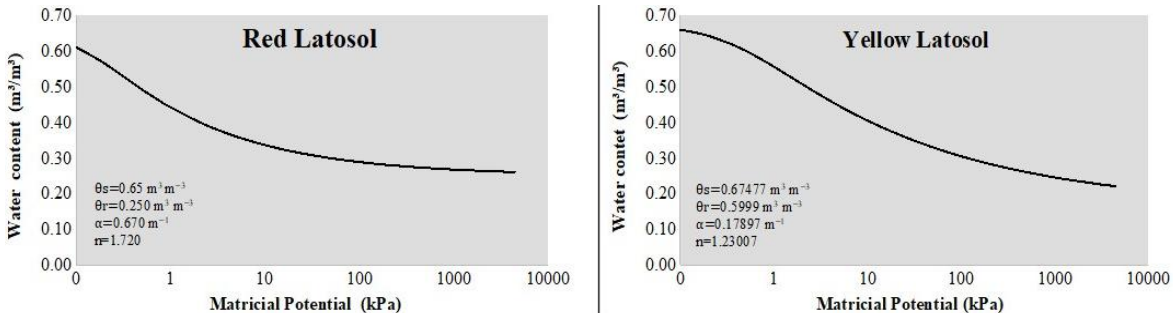

Figure 1. Soil water retention curve for the Red Latosol (Oxisol) and Red-Yellow Latosol.

$$LI = (\theta\Psi - \theta)\, Z \tag{1}$$

Where LI is the irrigation depth required to raise the soil moisture of the first 20 cm of soil to the field capacity or soil water tension of interest (mm), θΨ is the volumetric water content at the tension of interest for the first twenty cm of soil ($cm^3\ cm^{-3}$) obtained with tensiometer and soil water retention curve, θ is the estimated current volumetric water content for the first twenty cm of soil ($cm^3\ cm^{-3}$), and Z is the 20 cm soil depth (mm).

$$TI = \frac{LI\ A}{Q\ Ea}\, 60 \tag{2}$$

Where TI is the irrigation period (min), LI is the irrigation depth required to raise the soil moisture of the first 20 cm of soil to the field capacity or soil water tension of interest (mm), A is the soil area per pot (m^2), Q is the irrigation system flow rate ($L\ h^{-1}$), and Ea is the application efficiency (decimal number).

The CWSI was calculated using thermal images of the bean canopy. These images were obtained by a portable thermal camera (model DS-2TPH10-3AUF, Hikvision). It was determined according to the methodology proposed by Idso *et al.* (1981), which considers the difference between the canopy temperature (T_c), obtained by the thermal infrared imagery, and the air temperature (T_a), obtained by the climatological station (Equation 3). Thermal infrared imagery was acquired on 80 plants, on alternate days between 11:30 am and 1:30 pm, for a total of 40 images.

$$CWSI = \frac{(T_c - T_a) - ((T_c - T_a)_{ll}}{(T_c - T_a)_{ul} - (T_c - T_a)_{ll}} \tag{3}$$

Where T_c is the canopy temperature extracted from the thermal infrared image which shows the range of leaf temperature at the time the image was captured, T_a is the average air temperature, $(T_c - T_a)_{ll}$ is the non-water-stressed baseline (NWSB) corresponding to the air temperature difference for a crop without water deficit, i.e., when the resistance to water loss is zero or corresponding to the wet surface temperature, and $(T_c - T_a)_{ul}$ is the upper-temperature baseline, i.e., the non-transpiring baseline corresponding to the air temperature difference when the canopy water loss resistance increases without limits or corresponding to the dry surface temperature.

The upper and lower temperatures were obtained by the maximum and minimum differences between canopy and air temperatures (T_c-T_a). The NWSB equation was obtained by linear regression of (T_c-T_a) against atmospheric vapor pressure deficit (VPD). The VPD was calculated using Equation 4.

$$VPD = 0.6108 * EXP\left(\frac{7.5 * T_a}{T_a + 237.3}\right) * \left(1 - \frac{RH}{100}\right) \quad (4)$$

Where RH is the relative humidity.

The growth stages of the bean (Figure 2) ranged from EM – emergence day, V4 – the vegetative stage between 18 and 24 DAE, R5 and R6 – floral induction and flowering between 25 and 38 DAE, R7 – pod formation between 39 and 46 DAE, R8 – seed and pod filling between 47 and 66 DAE, and R9 – physiological maturity between 67 and 75 DAE. Note that CWSI was not calculated during the physiological maturity stage (R9) due to the plant's senescence.

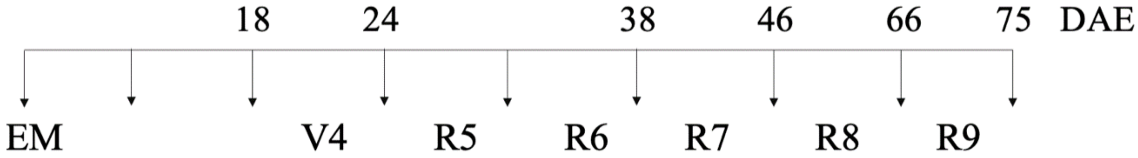

Figure 2. Growth stages of common bean (*Phaseolus vulgaris* L., cv BRSFC 104) cultivated in the greenhouse.

In the initial growth stages, some technical issues were experienced with the analogic pressure gauge, which later was changed to a digital pressure gauge with a silicone cap. It is suspected that some tensiometers had very small leaks, thus losing some vacuum. In addition, the shade net of the greenhouse created some interference with solar radiation and thus reduced light availability for the bean plants. All these factors may have influenced the SMP readings at the V4, R5 and R6 stages.

The relationship between (Tc-Ta) versus VPD, and CWSI against SMP and leaf water potential were analyzed by linear, non-linear, and multiple regressions. The statistical significance of the regressions was evaluated using the F-test, considering a significance level of 5% ($p \leq 0.05$). All statistical analyses were performed using R software (R Core Team, 2023) (version 4.0.4) and the ggplot2 package for graphical visualization.

3. RESULTS AND DISCUSSION

The NWSB was obtained from the vegetative stage (V4) to the seed and pod filling stage (R8). The linear regression models of the lower baseline plotted against VPD for Red Latosol, Red-Yellow Latosol are shown in Figures 3 and 4 respectively.

The Red-Yellow Latosol (R^2=0.62) presented a relatively strong and significant (p-value<0.001) relationship between (Tc-Ta) and VPD, whereas the Red Latosol showed a weaker (R^2= 0.37) but yet significant (p-value ≤ 0.001) relationship. The VPD values ranged from 1.18 to 2.87 kPa. The canopy temperature and air temperature difference (Tc-Ta) ranged from -0.38 to -12.22 ◦C; 0.12 to -11.29 ◦C for the Red Latosol and Red-Yellow Latosol, respectively.

Others studies have also determined the lower baseline for bean crops around the world under no stress conditions, yielding the following models with some level of similarity: Tc-Ta=2.79-1.59VPD; Tc-Ta=2.91-2.35 VPD; Tc-Ta=3.53-2.69 VPD; Tc-Ta=1,175-1,019 VPD.

In this experiment, we used climate data from 11:30 am to 1:30 pm. According to Erdem *et al.* (2006), the relationship can be affected by some factors such as clouds and wind, as well as incorrect readings of relative humidity. Many other factors such as cultivars, climatic conditions (including soil moisture), and growth stage also influence the upper baseline. In this respect, the different values in the regression equations developed for each soil type can be explained by the different capacities of these soils to retain and provide water for plants. Some researchers state that the no stress baseline may be fitted better when it is determined for each growth stage of the crop, in order to precisely represent the difference of (Tc-Ta) against VPD. This requires monitoring the VPD and relative humidity over the growing season and then plotting these data against (Tc-Ta).

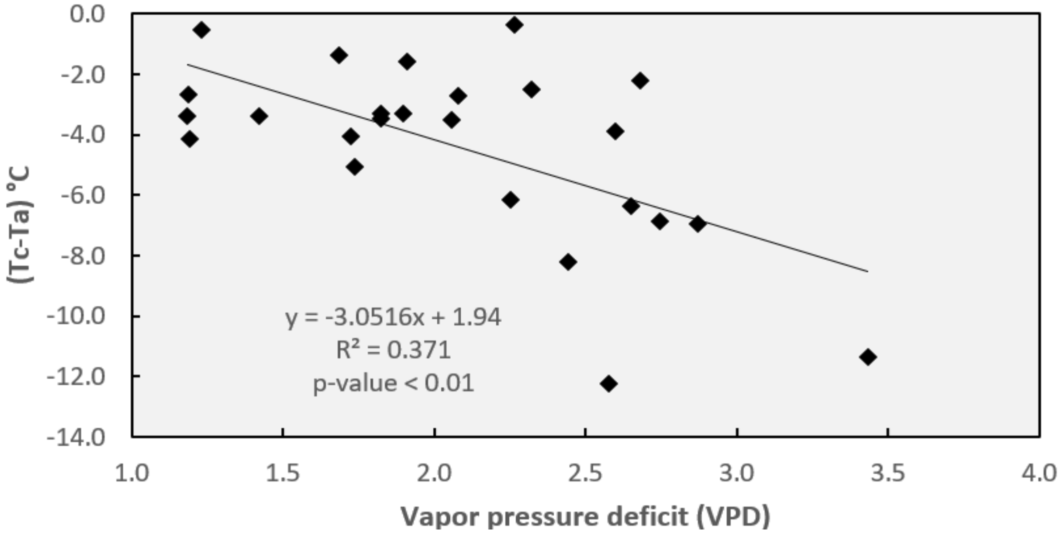

Figure 3. The non-water-stressed baseline (NWSB) for bean crop in the Red Latosol.

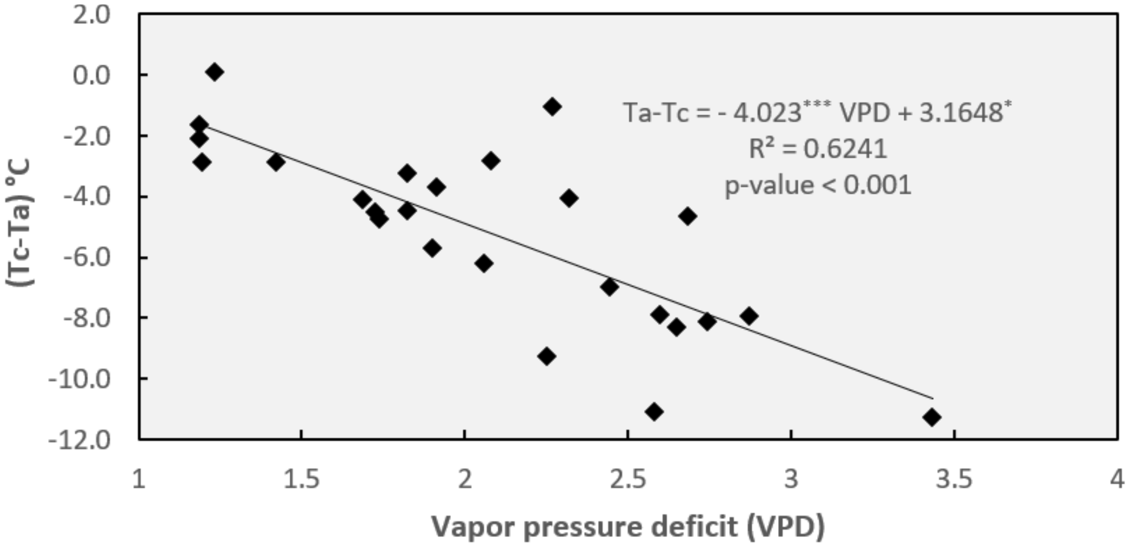

Figure 4. The non-water-stressed baseline (NWSB) for bean crop in the Red-Yellow Latosol.

3.1. Regression between CWSI and Soil Matric Potential

3.1.1. Red Latosol

Table 3 shows the R^2 and level of significance of the regression between the CWSI and soil matric potential for growth stages V4 to R8 of beans cultivated in the Red Latosol. Results suggest that regressions for V4, R5, R6 and R8 were not significant, whereas the regression was robust (R^2=0.8265) and significant (p-value = 0.032) for R7. For many of these models, here and for the other two soil types, the low degrees of freedom likely explain the low statistical significance of the regressions.

Table 3. Regression results of CWSI yielded for the four growth stages of bean in the Red Latosol.

Growth stage	Slips and Intercept	R^2	F	p-value
V4	$CWSI = 0.4898x^2 + 5.5072x + 15.8$	0.5585	1,265 on 2 and 2 DF	0.4415
R5 and R6	$CWSI = -0.1213x^2 - 1.8359x - 6.3056$	0.7065	2,407 on 2 and 2 DF	0.2935
R7	$CWSI = -0.0226x - 0.145$	0.8265	14.29 on 2 and 2 DF	0.0324
R8	$CWSI = -0.003x + 0.517$	0.2517	0.3364 on 2 and 2 DF	0.7483

*Significant at $p \leq 0.05$.

The highest CWSI was estimated at 0.82 and was associated with the treatment with the highest matric potential at R7 (Figure 5). For R5 and R6 stages, the relationship between the CWSI and soil matric potential was not significant, but the lowest CWSI value (0.20) was estimated in the treatment with the lowest soil matric potential (Figure 5). The regression coefficient was also high (R^2=0.70). The prediction of SMP in response to CWSI is shown in Table 4, a significant correlation was observed at stage R7 (R^2=0.84 and $p<0.05$). The correlation was weak and not significant for V4, R5, R6 and R8 stages.

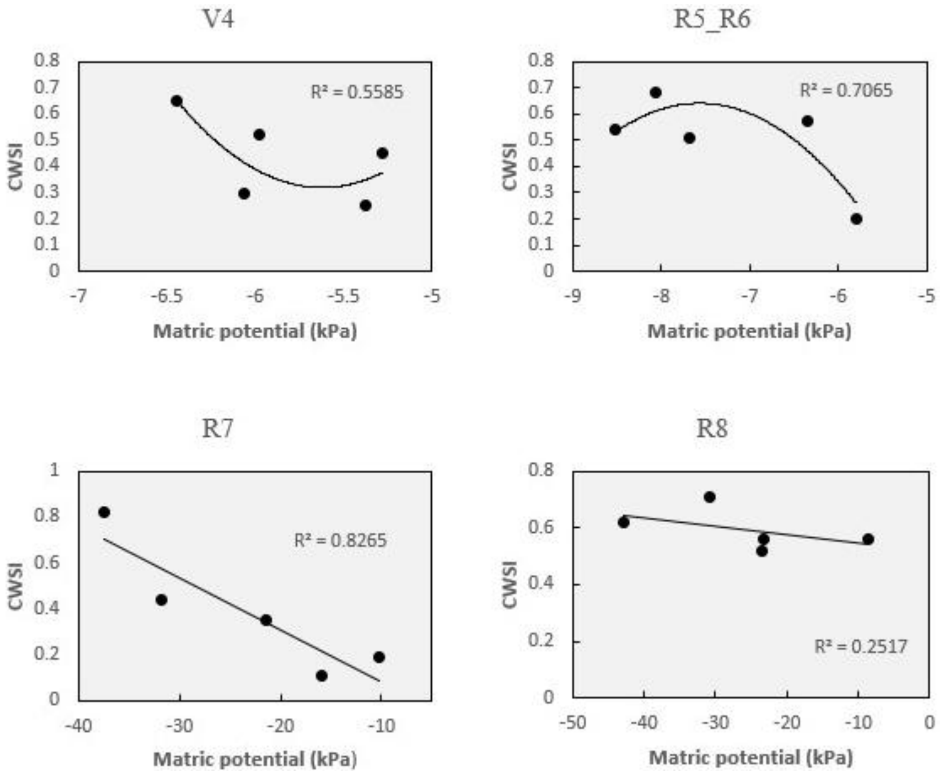

Figure 5. The CWSI plotted against the soil matric potential at different growth stages for beans in Red Latosol. V4 represents the vegetative stage, R5_R6 represents the flowering stage, R7 represents the pod formation stage, and R8 represents the seed and pod filling stage.

Table 4. SMP prediction in response to CWSI for the four growth stages of beans in Red Latosol.

Growth Stage	Slips and Intercept	R^2	p-value
V4	$KPA = -10.554x^2 + 7.5979x – 6.9136$	0.5136	> 0.05
R5 and R6	$KPA = 7. 349x^2 – 10.602x - 4.0059$	0.4969	> 0.05
R7	$KPA = 27.826x^2 – 63.067x - 5,0416$	0.8486	< 0.05
R8	$KPA = 786.58x^2 - 1058.2x + 321.76$	0.3148	> 0.05

The results in general showed that CWSI and soil water potential are correlated. The low availability of water in the soil resulted in high CWSI. This result corroborates with that of Silva *et al.* (2018) in tomatoes, where the treatments with the highest CWSI were found under water stress. The decrease in soil water content is the likely cause, as the plant reduces its transpiration by partially or totally closing its stomata. As a consequence, the canopy temperature tended to increase, and CWSI is the evidence. In general, a decrease in soil water content will tend to increase CWSI values, especially if air temperature and plant transpiration are measured near or at their peaks, e.g., at noon (Xu *et al.*, 2016).

Because soil moisture at R5 and R6 was high (Figure 5) and in turn, canopy temperature was low (or equilibrated), this result can be considered as evidence for an unstressed crop plant in regard to water. According to Xu *et al.*, (2016), under conditions where the CWSI value of rice was low and the plants did not suffer from water stress, soil water availability was sufficient to satisfy the plant's physiological processes. This particular state was reflected by low to moderate air temperature and thus relatively low water losses from evapotranspiration.

The regression between CWSI and soil matric potential for the various growth stages of bean cultivated in the Red-Yellow Latosol are presented in Table 5. We computed very strong and significant regressions at stages R5 and R6 (R^2=0.8566; p-value < 0.05) R7 (R^2=0.9795; p-value < 0.05) and R8 (R^2=0.9596; p-value < 0.05). For V4 stages, coefficient was high (respectively R^2=0.8354), but due to the low degrees of freedom, they were not statistically significant.

Table 5. Regression results of CWSI yielded for the four growth stages of bean in the Red-Yellow Latosol.

Growth Stage	Slips and Intercept	R^2	F-statistic	p-value
V4	CWSI = $0.5174x^2 + 5.8972x + 16,929$	0.8354	5,074 (3 and 1 DF)	0.1646
R5 and R6	CWSI = $0.0519x^2 + 1.0162x + 5,042$	0.8566	17.97 (1 and 3 DF)	0.0240
R7	CWSI = $0.0003x^2 - 0.0102x - 0.1531$	0.9795	47.84 on 2 and 2 DF	0.0205
R8	CWSI = $-0.0013x^2 - 0.0936x - 1.0083$	0.9596	23.77 on 2 and 2 DF	0.0404

*Significant at $p \leq 0.05$.

At the R5 and R6 stages, the highest CWSI value (0.84) and the lowest was found in the treatment with the lowest soil water content (Figure 6). The lowest and highest CWSI values at stage R7 were respectively estimated under the lowest and highest soil matric potential treatments, i.e., 0.07 and 0.69 (Figure 6). At the R8 stage, the lowest CWSI value was 0.19 and this was also related to the lowest soil matric potential (Figure 6). Table 6 shows SMP prediction equations in response to CWSI; a very strong and significant correlation was observed at the R8 stage (R^2 = 0.98 and p<0.05), whereas V4, R5 and R6, and R7 showed good correlation (R^2 > 0.62), but they were not significant.

These CWSI results at R5 to R8 (Figure 6) suggest that canopy temperature is sensitive to soil water availability, i.e., when water availability decreases, leaf temperature increases. The same observations between CWSI and canopy temperature under an irrigation gradient were made by Quiloango-Chimarro *et al.*, (2021) in common beans. Our results also corroborate with Bijanzadeh *et al.*, (2022) who found, for canola and sunflower crops, respectively, the lowest CWSI values under the irrigated treatment and the highest values under the water stress treatment.

Nouri *et al.* (2020) observed that the relationship between CWSI and soil moisture in bean crops under different irrigation treatments was negative and significant. The highest value of CWSI was found under the treatment representing the more severe water stress, i.e., the treatment with less irrigation, whereas the lowest CWSI value was found in the treatment receiving full irrigation.

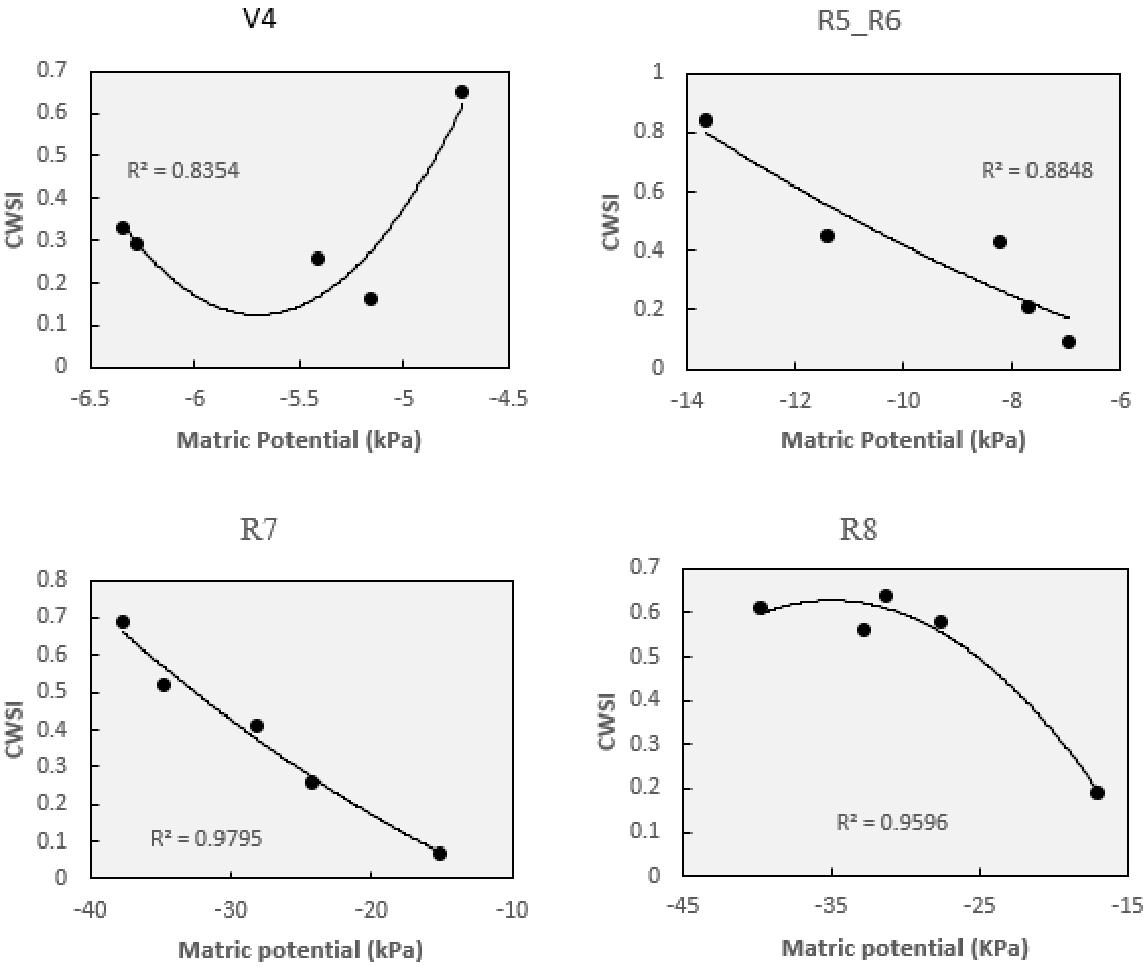

Figure 6. The CWSI plotted against the soil matric potential at different growth stages for beans in Red-Yellow Latosol. V4 represents the vegetative stage, R5_R6 represents the flowering stage, R7 represents the pod formation stage, and R8) represents the seed and pod filling stage.

Table 6 . SMP prediction in response to CWSI for the four growth stages of beans in Red-Yellow Latosol.

Growth Stage	Slips and Intercept	R²	p-value
V4	KPA = 23.137x ^{2} – 18.107x – 2.7391	0.8453	> 0.05
R5 and R6	KPA = -24.071x ^{2} + 17.604x – 11.187	0.6221	> 0.05
R7	KPA = 21.072x ^{2} – 52.946x – 11.497	0.9856	< 0.05
R8	KPA = 25.82x ^{2} – 59.382x - 6.6149	0.7332	> 0.05

According to Asemanrafat and Honar, (2017), the CWSI is conducive to change under different treatments, and CWSI is also affected by irrigation depths. They found that the treatments closest to the field capacity of the soil should have CWSI values closer to zero as the result of the regular supply of water. Under conditions of water stress, however, CWSI values should tend towards a value of 1.

The leaf water potential measurements were conducted at R8 (seed and pod filling stage). The regressions between CWSI and leaf water potential for Red Latosol and Red-Yellow Latosol are shown in Figure 7.

For Red Latosol (R^2=0.87) and Neosol (R^2=0.92) the regression was strong, while for Yellow-Red Latosol the correlation was weak, but not significant (p-value >0.05) for all soil types in this study.

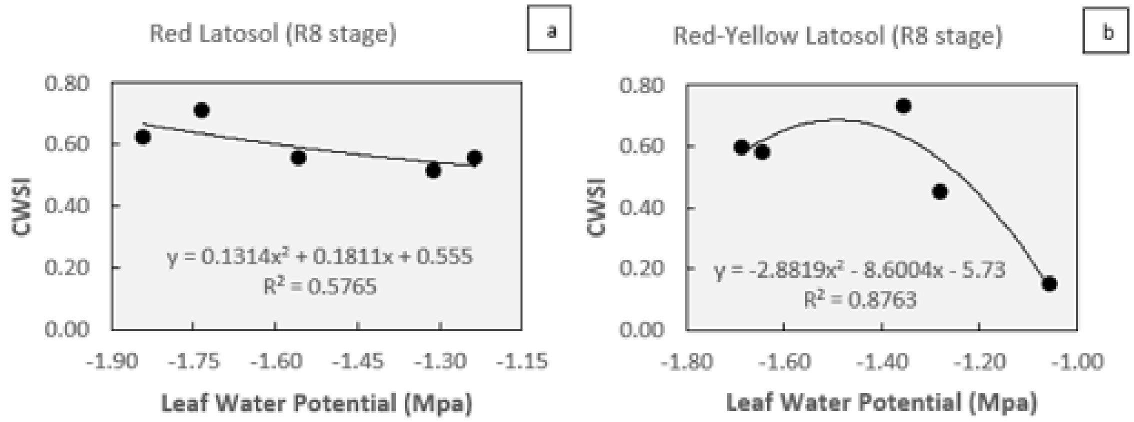

Figure 7. The CWSI against Leaf Water Potential at R8 stage for beans in different soil types: (a) Red Latosol, (b) and Red-Yellow Latosol.

According to our results, CWSI increases as LWP decreases, which is consistent with the results of Shellie and King (2020). For Red Latosol, the treatments under irrigation deficit showed the lowest values of leaf water potential, which are associated with the highest CWSI values. These results corroborate with those found by Kirnak *et al.*, (2019) who observed that the correlation between CWSI and LWP for pumpkin was strong (R^2=0.98 in 2015 and R^2=0.96 in 2016). The same behavior was found for the Red-Yellow Latosol, except for the high moisture treatment (10kPa), where the LWP was the same as the very dry treatment (40kPa). Wijewardana *et al.*, (2019) reported that the LWP decreased as the soil moisture decreased.

The multiple regression equations were extracted for the parameters of CWSI, soil matric potential and leaf water potential, in order to better understand these relations of plant and soil indices with CWSI. The results showed a good relationship for all studied soils, for the Red Latosol (R^2=0.69) and the Red Yellow (R^2=0.75), but none of the regressions were significant.

The strong correlation found between CWSI and leaf water potential (LWP) at stage R8 (Figure 7) reinforces that the thermal index is a reliable indicator of the plant's internal water status, as suggested by Kirnak *et al.* (2019) for other crops.

Table 7 shows the models for predicting CWSI for Red Latosol and Yellow-Red Latosol in response to LWP.

Table 7. Multiple regression models and multiple R-squared for predicting CWSI at phase R8 in beans.

Type of soil	models	R^2
Red Latosol	CWSI = 0.0751951 - 0.0057555 * KPA - 0.4241548 * PFOLIAR - 0.0003614 * KPA*PFOLIAR	0.69
Red yellow Latosol	CWSI = -0.271972 + 0.021511 * KPA - 0.261347 * PFOLIAR + 0.007366 *KPA*PFOLIAR	0.77

The results showed the potential of CWSI to predict KPA for Red and Yellow Latosols at R7. When calibrated in controlled conditions by a plant water indicator such as the leaf water potential and soil matric potential, the CWSI can be used to predict water stress in plants and be used as an indicator for scheduling irrigation and water management in agriculture, especially in areas where there are limitations for site measurements.

Studies have been showing the effectiveness of plant predictions based on calibrated models in a controlled environment (Pradawet *et al.*, 2022), and how it can lead to improved crop water management for different crops, soil, and climate conditions. In a controlled environment the monitoring the plants, soil and climate parameters can be done according to given purposes for different scenarios, i.e., assessing water stress applying different irrigation depths, at growth stages, periods of the day, reducing meteorological influences. Once it is calibrated and validated it can be used in fields as a reliable method.

The prediction regression models in this study demonstrated the higher applicability of CWSI to monitor the levels of stress in plants, mainly, when correlated to SMP.

4. CONCLUSION

The CWSI based on canopy temperature appears to be an effective tool to determine irrigation requirements in common beans considering their growth stages. In this study, significant curvi-linear regressions between the soil matric potential and CWSI were found for Red Latosol at growth stage R7 and for Yellow-Red Latosol at stages R5 to R8.

These results demonstrated good correlations between CWSI and soil matric potential, and the capability of prediction of soil matric potential using CWSI.

Prediction equations can be used to estimate the CWSI and soil matric potential as a means to monitor water deficit in plants. These can be used to better define irrigation needs in beans and thus develop more precise irrigation management plans.

5. DATA AVAILABILITY STATEMENT

Data availability not informed.

6. ACKNOWLEDGEMENTS

This study was funded by CNPQ (chamada MCTIC/CNPq Nº 28/2018, Process: 423744/2018-6).

This research was financially supported by DPI/BCE/UnB (University of Brasília), under Public Notice No. 001/2026.

7. REFERENCES

ASEMANRAFAT, M.; HONAR, T. Effect of water stress and plant density on canopy temperature, yield components and protein concentration of red bean (*Phaseolus vulgaris* l. Cv. Akhtar). **International Journal of Plant Production,** v. 11, p. 241–258, 2017.

BELLVERT, J.; ZARCO-TEJADA, P. J.; GIRONA, J.; FERERES, E. Mapping crop water stress index in a “Pinot-noir” vineyard: comparing ground measurements with thermal remote sensing imagery from an unmanned aerial vehicle. **Precision Agriculture**, v. 15, n. 4, p. 361–376, 2014. https://doi.org/10.1007/s11119-013-9334-5

BIJANZADEH, E.; MOOSAVI, M. M.; BAHADORI, F. Quantifying water stress of safflower (Carthamus tinctorius L.) cultivars by crop water stress index under different irrigation regimes. **Heliyon,** v. 8, n. 3, 2022. https://doi.org/10.1016/j.heliyon.2022.e09010

CONAB. **Série histórica de monitoramento de grãos por produtos**. Dezembro, 2023. Available at: https://www.conab.gov.br/info-agro/safras/serie-historica-das-safras. Access: 22 dez. 2024.

ERDEM, Y.; ŞEHIRALI, S.; ERDEM, T.; KENAR, D. Determination of crop water stress index for irrigation scheduling of beans (*phaseolus vulgaris l.).* **Turkish Journal of Agriculture and Forestry,** v. 30, n. 3, p. 195, 2006.

GONZÁLEZ-DUGO, V.; ZARCO-TEJADA, P. J.; NICOLÁS, E.; NORTES, P. A.; ALARCÓN, J. J.; INTRIGLIOLO, D. S. *et al.* Using high resolution UAV thermal imagery to assess the variability in the water status of five fruit tree species within a commercial orchard. **Precision Agriculture,**v. 14, p. 660-678, 2013. https://doi.org/10.1007/s11119-013-9322-9

IDSO, S. B.; JACKSON, R. D.; PINTER JÚNIOR, P. J.; REGINATO, R. J.; HATFIELD, J. L.; Normalizing the stress-degree-day parameter for environmental variability. **Agricultural Meteorology,** v. 24, p. 45-5, 1981. https://doi.org/10.1016/0002-1571(81)90032-7

JACKSON, R. D.; IDSO, S. B.; REGINATO, R. J.; PINTER, P. J. J. Canopy temperature as a crop water stress indicator. **Water Resources Research,** v. 17, p. 1133-1138, 1981. https://doi.org/10.1029/WR017i004p01133

LOBO, F. A.; OLIVA, M. A.; RESENDE, M.; LOPES, N. F.; MAESTRI, M. Termometria ao infravermelho na programação da irrigação de feijoeiro. **Pesquisa Agropecuária Brasileira,** v. 39, n. 2, p. 113-121, 2004. https://doi.org/10.1590/S0100-204X2004000200003

OLIVEIRA, L. F. C.; OLIVEIRA, R. Z.; CASTRO, T. A. P. Comportamento fisiológico de cafeeiros submetidos a diferentes disponibilidades de água no solo. **Bioscience Journal,** v. 25, n. 3, p. 83-91, 2009.

KIRNAK, H.; IRIK, H. A.; UNLUKARA, A. Potential use of crop water stress index (CWSI) in irrigation scheduling of drip-irrigated seed pumpkin plants with different irrigation levels. **Scientia Horticulturae**, v. 256, 2019. https://doi.org/10.1016/j.scienta.2019.108608

NOURI, S.; NASROLAHI, A.; MALEKI, A.; SHARIFIPOUR, M. Estimation of soil moisture content using crop water stress index for irrigation management of pinto bean. **Iranian Journal of Irrigation and Drainage,** v. 1, n. 14, p. 136-145, 2020.

PADHI, J.; MISRA, R. K.; PAYERO, J. O. Estimation of soil water deficit in an irrigated cotton field with infrared thermography. **Field Crops Research,** v. 126, p. 45-55, 2012. https://doi.org/10.1016/j.fcr.2011.09.015

PEREIRA, R. M. **Manejo de irrigação com automação de baixo custo no cultivo da alface submetida a diferentes potenciais matriciais do solo**. 2021. 118p. Tese (doutorado em agronomia) – Universidade de Brasília, Faculdade de Agronomia e Medicina Veterinária, Brasília, 2021.

PRADAWET, C.; KHONGDEE, N.; HILGER, T.; CADISCH, G. Thermal imaging for assessment of maize water stress and yield prediction under drought conditions. **Journal of Agronomy and Crop Science,** v. 209, p. 56-70, 2022. https://doi.org/10.1111/jac.12582

QUILOANGO-CHIMARRO, C.; COELHO, R. D.; COSTA, J. DE O.; GOMEZ-ARRIETA, R. Crop water stress index for predicting yield loss in common bean**. Irrigation,** v. 1, n. 4, p. 687–695, 2021. http://dx.doi.org/10.15809/irriga.2021v1n4p687-695

R CORE TEAM. **R**: A language and environment for statistical computing. Vienna: R Foundation for Statistical Computing, 2023.

SHELLIE, K. C.; KING, B. A. Application of a Daily Crop Water Stress Index to Deficit Irrigate Malbec Grapevine under Semi-Arid Conditions. **Agriculture,** v. 10. n. 492, 2020. http://dx.doi.org/10.3390/agriculture10110492

SILVA, C. J.; SILVA, C. A.; FREITAS, C. A.; GOLYNSKI, A.; SILVA, L. F. M.; FRIZZONE, J. A., Tomato water stress index as a function of irrigation depths**. Revista Brasileira de Engenharia Agrícola e Ambiental,** v. 22, n. 2, p. 95-100, 2018. http://dx.doi.org/10.1590/1807-1929/agriambi.v22n2p95-100

VAN GENUCHTEN, M. T. A closed-form equation for predicting the hydraulic conductivity of unsaturated soils. **Soil Science Society of America Journal**, v. 44, p. 892-898, 1980.

WIJEWARDANAA, C.; ALSAJRIA, F. A.; IRBYA, I. T.; KRUTZ, L. J.; COLDENC, B.; HENRYA, W. B. *et al.* Physiological assessment of water deficit in soybean using midday leaf water potential and spectral features. **Journal of plant interactions,** v. 14, n. 1, p. 533–543, 2019. https://doi.org/10.1080/17429145.2019.1662499

XU, J.; LV, Y.; LIU, X.; DALSON, T.; YANG, S.; WU, J. Diagnosing crop water stress of rice using infra-red thermal imager under water deficit condition. **International Journal of Agricultural Biology**, v. 18, p. 565–572, 2016. http://dx.doi.org/10.17957/ijab/15.0125